

# Adaptive Control for Energy Storage Systems in Households With Photovoltaic Modules

Yanzhi Wang, *Student Member, IEEE*, Xue Lin, *Student Member, IEEE*, and Massoud Pedram, *Fellow, IEEE*

**Abstract**—Integration of residential-level photovoltaic (PV) power generation and energy storage systems into the smart grid will provide a better way of utilizing renewable power. With dynamic energy pricing models, consumers can use PV-based generation and controllable storage devices for peak shaving on their power demand profile from the grid, and thereby, minimize their electric bill cost. The residential storage controller should possess the ability of forecasting future PV power generation as well as the power consumption profile of the household for better performance. In this paper, novel PV power generation and load power consumption prediction algorithms are presented, which are specifically designed for a residential storage controller. Furthermore, to perform effective storage control based on these predictions, the proposed storage control algorithm is separated into two tiers: the global control tier and the local control tier. The former is performed at decision epochs of a billing period (a month) to globally “plan” the future discharging/charging schemes of the storage system, whereas the latter one is performed more frequently as system operates to dynamically revise the storage control policy in response to the difference between predicted and actual power generation and consumption profiles. The global tier is formulated and solved as a convex optimization problem at each decision epoch, whereas the local tier is analytically solved. Finally, the optimal size of the energy storage module is determined so as to minimize the break-even time of the initial investment in the PV and storage systems.

**Index Terms**—Control, energy storage, photovoltaic, prediction.

## I. INTRODUCTION

THE traditional static and centralized structure of electricity grid is comprised of a transmission network, which transmits electrical power generated at remote power plants through long-distance high-voltage lines to substations, and a distribution network, which delivers electrical power from substations to local end users. Since the end user profiles often significantly change according to the day of week and time of day, the power grid must be able to support the worst-case demand of power to all end users [1].

The smart grid infrastructure is being designed to avoid expending a large amount of capital for increasing the power generation capacity of utility companies in order to meet the expected growth of end user energy consumption at the worst case [2]. The smart grid is integrated with smart meters, which can

monitor and control the power flow in the Grid to match the amount of power generation to that of power consumption, and to minimize the overall cost of electrical power delivered to the end users. Utility companies can employ *dynamic electricity pricing* strategies, incentivizing consumers to perform *demand side management* by adjusting their loads to match the current state of the network, i.e., shifting their loads from the peak periods to off peak periods. There are several ways to perform demand side management, including integration of renewable energy sources such as photovoltaic (PV) power or wind power at the residential level, demand shaping, and so on [3]. In this paper, we focus on the former solution, or more specifically, integrating PV power generation with the smart grid for residential usage.

Although integrating residential-level renewable energy sources into the smart grid proves useful in reducing the usage of fossil fuels, several problems need to be addressed for these benefits to be realized. First, there exists a mismatch between the peak PV power generation time (usually at noon) and the peak load power consumption time for the residential user (usually in the evening.) This timing skew results in cases where the generated PV power cannot be optimally utilized for peak power shaving. Moreover, at each time instance, the PV output power is fixed, depending on the solar irradiance [4]. Hence, the ability of the residential user for peak shaving is also restricted by the PV output power.

An effective solution of the above-mentioned problems is to incorporate an *energy storage module* for houses equipped with PV modules [5]. The proposed residential energy storage module stores power from the smart grid during off peak periods of each day and (or) from the PV system, and provide power for the end users during the peak periods of that day for peak power shaving and energy cost reduction (since electrical energy tends to be the most expensive during these peak hours.) Therefore, the design of energy pricing-aware control algorithm for the residential storage system, which controls the charging and discharging of the storage and the magnitude of the charging/discharging current, is an important task in order for the smart grid technology to deliver on its promises.

A realistic electricity pricing function [9] consists of both an *energy price* component, which is a time of usage (TOU) dependent function indicating the unit energy price during each time period of the billing period (a day, or a month, etc.), and a *demand price* component, which is an additional charge due to the peak power consumption in the billing period. The latter component is added to the price of energy consumption in order to prevent a case whereby all customers utilize their PV power generation and energy storage systems and/or schedule their loads such that a very large amount of power is demanded from the smart grid during low-cost time slots, which can subsequently result in the power delivery failure.

Manuscript received February 16, 2013; revised July 17, 2013; accepted October 25, 2013. Date of publication February 03, 2014; date of current version February 14, 2014. This research is sponsored in part by grants from the Software and Hardware Foundations of the Division of Computer and Communication Foundations of the U.S. National Science Foundation. A preliminary version of this paper was presented at the 2012 IEEE Green Technologies Conference (GTC), Tulsa, OK, USA [5]. Paper no. TSG-00174-2013.

The authors are with the Department of Electrical Engineering, University of Southern California, Los Angeles, CA 90089 USA (e-mail: yanzhiwa@usc.edu, xuelin@usc.edu, pedram@usc.edu).

Color versions of one or more of the figures in this paper are available online at <http://ieeexplore.ieee.org>.

Digital Object Identifier 10.1109/TSG.2013.2292518

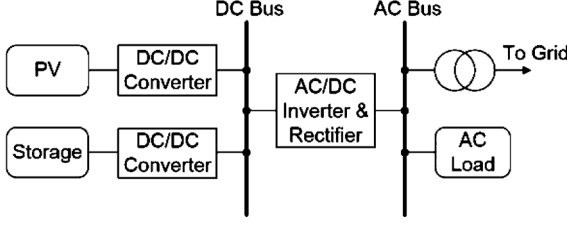


Fig. 1. Block diagram showing the interface between PV module, storage system, residential load, and the smart grid.

Moreover, the size of the storage system is limited due to the relatively high cost of electrical energy storage elements. Therefore, at each decision epoch (some predefined time instances for the storage controller to make decisions) of a billing period, it is important for the controller to forecast the future PV power generation and load power consumption profiles so that it can perform optimization of the total cost. References [6]–[8] are representative of PV power generation and load power consumption profile predictions by either predicting the whole power profiles, or predicting certain statistical characteristics. However, these methods are general profile predicting methods, not specifically designed to help a residential storage controller. The controller may not perform the optimal electrical energy cost reduction over each billing period by using such prediction methods.

In this paper, we consider the case of a residential smart grid user equipped with a local PV power generation module and an energy storage module. We consider a realistic electricity price function comprised of both energy and demand prices. First, we present novel PV power generation and load power consumption profile predictors specifically designed for the residential smart grid controller. The predictors exploit the specific form of the energy price function, and effectively avoid underestimation of the load power consumption or overestimation of the PV power generation. Furthermore, to perform effective and adaptive storage control utilizing these prediction results to minimize the total energy cost, we decompose the proposed control algorithm into a *global control tier* and a *local control tier*. The global control tier is performed at each decision epoch of the billing period to globally “plan” the future discharging and charging schemes of the storage system, whereas the local control tier is performed along with system operation to compensate the prediction errors. The global tier is effectively implemented by solving a convex optimization problem at each decision epoch, whereas the local tier has a time complexity of  $O(1)$ . We find the optimal size of the energy storage module so as to minimize the break-even time of the initial investment in the PV and storage systems.

## II. SYSTEM MODEL AND COST FUNCTIONS

In this paper, we consider a residential smart grid user equipped with PV power generation and energy storage modules as shown in Fig. 1. The PV and storage modules are connected to a (residential) *DC bus* via DC-DC converters. An *AC bus*, which is further connected to the smart grid, is connected to the DC bus via AC/DC inverter and rectifier. The residential *AC load* is connected to the AC bus.

We adopt a *slotted time* model, i.e., all system constraints as well as decisions are provided for discrete time intervals of equal and constant length. Each day is divided into  $T$  time slots, each of duration  $D$ . We use  $T = 96$  and  $D = 15$  minutes.

We adopt a realistic electricity price function comprising both the energy price component and the demand price component,

with a billing period of a month [9]. Consider a specific day  $i$  of a billing period. The residential load power consumption at the  $j$ th time slot of that day is denoted by  $P_{\text{load},i}[j]$ . The output power levels of the PV and storage systems at the  $j$ th time slot are denoted by  $P_{\text{pv},i}[j]$  and  $P_{\text{st},i}[j]$ , respectively, where  $P_{\text{st},i}[j]$  can be positive (discharging the storage), negative (charging the storage), or zero. Therefore, the power drawn from the smart grid, i.e., the *grid power*, at the  $j$ th time slot of the  $i$ th day is:

$$P_{\text{grid},i}[j] = P_{\text{load},i}[j] - P_{\text{pv},i}[j] - P_{\text{st},i}[j] \quad (1)$$

where  $P_{\text{grid},i}[j]$  can be positive (if the smart grid provides power for the residential usage), negative (if the residential user sells power back into the smart grid), or zero.

As specified in [9], the electricity price function is pre-announced by the utility company just before the start of each billing period, and the price function will not change until possibly the start of the next billing period. Reference [9] also specifies five different time periods of each day, denoted by the term *price periods*, with (potentially) different unit energy prices and (or) demand prices. These pre-announced price periods are: the 1st off peak (OP) period from 00:00 to 09:59, the 1st low peak (LP) period from 10:00 to 12:59, the high peak (HP) period from 13:00 to 16:59, the 2nd LP period from 17:00 to 19:59, and the 2nd OP period from 20:00 to 23:59. For notation simplicity, we denote the 1st OP, 1st LP, HP, 2nd LP, and 2nd OP price periods of a day as the 1st, 2nd, 3rd, 4th, and 5th price periods of that day. We use  $j \in S_k$  to denote the statement that the  $j$ th time slot belongs to the  $k$ th price period. We use  $t_{s,k}$  and  $t_{e,k}$  to denote the start time and end time of the  $k$ th price period in each day, respectively. We have  $t_{s,1} = 00 : 00$  (start time of the day),  $t_{e,5} = 23 : 59$  (end time of the day), and  $t_{s,k} = t_{e,k-1}$  for  $2 \leq k \leq 5$ .

We use  $\text{Price}_{E_{\text{OP}}}$ ,  $\text{Price}_{E_{\text{LP}}}$ , and  $\text{Price}_{E_{\text{HP}}}$  to denote the unit energy price in the OP period (the 1st and 5th price periods), the LP period (the 2nd and 4th price periods), and the HP period (the 3rd price period) of each day, respectively, and use  $\text{Price}_{D_{\text{LP}}}$ ,  $\text{Price}_{D_{\text{HP}}}$ , and  $\text{Price}_{D_{\text{Overall}}}$  to denote the monthly demand price for the peak power demands drawn from the Grid during the LP period, the HP period, and the overall peak power demand of a billing period (a month), respectively. We have  $\text{Price}_{E_{\text{HP}}} > \text{Price}_{E_{\text{LP}}} > \text{Price}_{E_{\text{OP}}}$  and  $\text{Price}_{D_{\text{HP}}} > \text{Price}_{D_{\text{LP}}}$ . The cost we pay in a billing period due to the energy price component is given by:

$$\begin{aligned} \text{Cost}_E &= \text{Price}_{E_{\text{OP}}} \cdot \sum_{i=1}^{30} \sum_{j \in S_1 \cup S_5} P_{\text{grid},i}[j] \cdot D \\ &+ \text{Price}_{E_{\text{LP}}} \cdot \sum_{i=1}^{30} \sum_{j \in S_2 \cup S_4} P_{\text{grid},i}[j] \cdot D \\ &+ \text{Price}_{E_{\text{HP}}} \cdot \sum_{i=1}^{30} \sum_{j \in S_3} P_{\text{grid},i}[j] \cdot D \quad (2) \end{aligned}$$

and the cost we pay in the billing period due to the demand price component is given by

$$\begin{aligned} \text{Cost}_D &= \text{Price}_{D_{\text{LP}}} \cdot \max_{1 \leq i \leq 30, j \in S_2 \cup S_4} P_{\text{grid},i}[j] \\ &+ \text{Price}_{D_{\text{HP}}} \cdot \max_{1 \leq i \leq 30, j \in S_3} P_{\text{grid},i}[j] \\ &+ \text{Price}_{D_{\text{Overall}}} \cdot \max_{1 \leq i \leq 30, 1 \leq j \leq 96} P_{\text{grid},i}[j] \quad (3) \end{aligned}$$

The total cost for the residential user in the billing period is the sum of the two aforesaid cost components.

### III. PV AND LOAD POWER PROFILE PREDICTION

Accurate prediction of the PV power generation and load power consumption profiles is extremely important for the development of residential storage control algorithms. Due to the fact that predicting the complete load (or PV) power profile is difficult and unnecessary (since the storage controller only needs certain characteristics of the load or PV power profiles, e.g., average values and magnitudes and time instances of peaks), we use predictors to forecast the peak and average load power consumption (or PV power generation) values for *different price periods in each day*, i.e., one predictor for the 1st OP period, one for the 1st LP period, one for the HP period, one for the 2nd LP period, and one for the 2nd OP period. Subsequently, we reconstruct the approximate load (or PV) power profile for each day based on the predicted average and peak values in each price period.

In the following, we describe the peak power predictors. The average predictors, which tend to be more accurate, are realized by using the same algorithms. The proposed load power consumption and PV power generation prediction algorithms consist of an *initial prediction* phase followed by an *intra-day refinement* phase, as explained below.

Consider the peak power (consumption or generation) prediction for the  $i$ th day of a billing period (i.e., a month.) The initial prediction of the peak power refers to the prediction performed at time 00:00 ( $t_{s,1}$ ) of the  $i$ th day, for the peak load power consumption (or PV power generation) in all five price periods of the  $i$ th day. The intra-day refinement of peak power (consumption or generation) prediction may be performed at the start time of the  $k$ th ( $1 < k \leq 5$ ) price periods, i.e.,  $t_{s,k}$ , of the  $i$ th day, with the goal of refining the initial prediction results in the  $k$ th,  $(k+1)$ st, ..., 5th price periods.

Motivation for the intra-day refinement is that at time  $t_{s,k}$  ( $1 < k \leq 5$ ), the actual peak load power consumption (or PV power generation) values in the 1st, 2nd, ...,  $(k-1)$ st price periods of the  $i$ th day are known to the controller. This information can thus be used to improve the accuracy of peak power prediction for the rest of price periods in the same day. The proposed intra-day refinement process is crucial since the characteristics of the load power consumption and PV power generation profiles are required to be more accurate for the 1st LP, HP, and 2nd LP periods compared to the 1st OP period. This is because the energy and demand prices in the former price periods are higher than those for the 1st OP price period. In addition, it is very unlikely for the peak power demand from the Grid to occur during the 1st OP period.

#### A. Prediction for the Peak Load Power Consumption

For the initial prediction phase of peak load power consumption, an adaptive regression-based algorithm is used. Consider that we are at time  $t_{s,1} = 00 : 00$  of the  $i$ th day. The peak load power consumption values in the  $k$ th price period of the  $i$ th day ( $1 \leq k \leq 5$ ) are predicted as follows:

$$\text{Predict}_{i,k} = \sum_{l=1}^n \theta_{i,k}(l) \cdot \text{Feature}_{i,k}(l) \quad (4)$$

where the feature vector  $\text{Feature}_{i,k} = (\text{Feature}_{i,k}(1), \text{Feature}_{i,k}(2), \dots, \text{Feature}_{i,k}(n))$

captures the actual values of peak load power consumption sampled at some previous points of interest, and  $n$  is the number of elements in the feature vector. In addition,  $\theta_{i,k} = (\theta_{i,k}(1), \dots, \theta_{i,k}(n))$  denotes a dynamically-updated coefficient vector with  $n$  elements. The values of elements  $\theta_{i,k}(1), \dots, \theta_{i,k}(n)$  are all initialized to  $1/n$ . Utilizing a stochastic gradient descent method (see [10] for details), the coefficient vector  $\theta_{i,k}$  is updated as follows:

$$\theta_{i+1,k} \leftarrow \theta_{i,k} + \alpha \cdot (\text{Actual}_{i,k} - \text{Predict}_{i,k}) \cdot \text{Feature}_{i,k} \quad (5)$$

where  $0 < \alpha < 1$  is a pre-defined *learning parameter*.

Testing on the load power consumption profile from Baltimore Gas and Electric Company [11], we have found that a value of  $n = 5$  with the feature vector defined as follows yields the best prediction results with a relatively low computational complexity (a overlarge  $n$  will result in not only high computation complexity but also over-fitting [10]):

$$\text{Feature}_{i,k} = (\text{Actual}_{i-1,k}, \text{Actual}_{i-2,k}, \text{Actual}_{i-7,k}, \text{Actual}_{i-14,k}, \text{Actual}_{i-21,k}) \quad (6)$$

where the  $\text{Actual}_{*,k}$  values denote the actual peak load power consumption values in the  $k$ th price period of the  $(i-1)$ st day, the  $(i-2)$ nd day, the  $(i-7)$ th day, the  $(i-14)$ th day, and the  $(i-21)$ st day, respectively. This is because the tested load power profile exhibits both daily dependency and weekly dependency. The daily dependency is properly captured by the feature elements of the  $(i-1)$ st day and the  $(i-2)$ nd day, whereas the weekly dependency is captured by those of the  $(i-7)$ th day, the  $(i-14)$ th day, and the  $(i-21)$ st day.

For the intra-day refinement phase of peak load power consumption prediction, consider that we are currently at time instance  $t_{s,k}$  (the start time of the  $k$ th price period) of day  $i$ , and we intend to refine the initial prediction results of the peak load power consumption values in the  $\hat{k}$ th ( $k \leq \hat{k} \leq 5$ ) price period of that day. We denote the result of refinement as  $\text{Refine}_{i,\hat{k}}$ . Since at that time  $t_{s,k}$  the actual peak load power consumption in the  $(k-1)$ st price period is already known, we calculate  $\text{Refine}_{i,\hat{k}}$  as follows:

$$\text{Refine}_{i,\hat{k}} \leftarrow (1 - \gamma) \text{Predict}_{i,\hat{k}} + \gamma \cdot \frac{\text{Actual}_{i,k-1}}{\text{Predict}_{i,k-1}} \cdot \text{Predict}_{i,\hat{k}} \quad (7)$$

where the coefficient  $0 < \gamma < 1$ . We learn the optimal  $\gamma$  value using the same stochastic gradient descent method (see [10] for details) as the learning process of the coefficient vector  $\theta_{i,k}$ . Typically, a  $\gamma$  value in the range of [0.5, 0.7] will yield the best prediction results.

The intuition for this update equation (7) is as follows: If the actual peak load power consumption in the  $(k-1)$ st price period is higher than the predicted peak load power consumption in that period, i.e.,  $\text{Actual}_{i,k-1} > \text{Predict}_{i,k-1}$ , it is highly likely that the actual load power consumption in the  $\hat{k}$ th price period ( $k \leq \hat{k} \leq 5$ ) of the same day will also be higher than the predicted peak load power consumption in that period, and vice versa. Experimental results in Section V will demonstrate that the prediction error can be reduced to 50% of the initial prediction error by using intra-day refinement.

It is important to note that underestimating peak load power consumption needs to be avoided, since it may result in larger

than expected power demand from the smart grid, which in turn significantly increases the monthly demand price of electricity. We propose to use the following heuristic for avoiding underestimation of peak load power consumption. We modify the afore-said intra-day refinement algorithm in that after we have derived the  $\text{Refine}_{i,\hat{k}}$  ( $2 \leq \hat{k} \leq 5$ ) value using (7), we add the following additional correction phase:

$$\text{Refine}_{i,\hat{k}} \leftarrow \text{Refine}_{i,\hat{k}} \cdot \eta_{\text{load}}, \quad \text{if } \text{Refine}_{i,\hat{k}} > \text{Predict}_{i,\hat{k}} \quad (8)$$

where the correction factor  $\eta_{\text{load}} > 1$ .

The reason for this modification is as follows. Experimental results show that underestimating peak load power consumption in the  $\hat{k}$ th price period of the  $i$ th day is very likely to occur when  $\text{Refine}_{i,\hat{k}} > \text{Predict}_{i,\hat{k}}$ .

We effectively learn the optimal correction factor  $\eta_{\text{load}}$  value using a simple learning technique [10] discussed as follows. We maintain a set of correction factors  $\{\eta_{\text{load},1}, \eta_{\text{load},2}, \dots, \eta_{\text{load},m}\}$  and pick one of them in each billing period. At the end of the billing period, we evaluate the cost-saving performance of the storage controller if each correction factor is chosen in this billing period, and find  $\eta_{\text{load},l}$  that results in the lowest energy cost. Then we select the correction factor  $\eta_{\text{load},l}$  in the next billing period.

#### B. Prediction Algorithm for the Peak PV Power Generation

For the peak PV power generation prediction, an important observation is that the actual peak PV power generation over a specific price period (e.g., the  $k$ th price period) in the  $i$ th day of a billing period may be viewed as the peak PV power generation over the  $k$ th price period for a sunny day, multiplied by a *decay factor*, representing the effect of clouds, if that day is cloudy. Obviously, such sunny day peak PV power generation over the  $k$ th period ( $1 \leq k \leq 5$ ) varies with the change in seasons. This effect is however captured by a *smoothing operation* as described below (cf. (9) and (10).) Therefore, we use the initial prediction, which is performed at the beginning of each day, mainly to *predict the sunny day peak PV power generation* over each price period of that day. Next, we rely on the intra-day refinement, which is performed at the start time of the  $k$ th ( $1 < k \leq 5$ ) price period  $t_{s,k}$  of that day, in order to predict the decay factors (and subsequently, the actual peak PV power generation levels) in the rest of price periods. Please note that at time  $t_{s,k}$ , the decay factor in the  $(k-1)$ st price period is already known. Moreover, decay factors for different price periods of the same day are positively correlated in general.

In the initial prediction phase, we adopt a variant of the well-known exponential average-based prediction method, in order for effectively predicting the sunny day peak PV power generation in each price period of day (please see the discussion below about how our version is different from the standard method.) Consider that we are at time  $t_{s,1} = 00 : 00$  of the  $i$ th day. We want to derive the prediction value of the sunny day peak PV power generation in the  $k$ th ( $1 \leq k \leq 5$ ) price period of that day, denoted by  $\text{Predict}_{i,k}$ , based on the prediction result of sunny day peak PV power generation value in the  $k$ th price period of the  $(i-1)$ st day, denoted by  $\text{Predict}_{i-1,k}$ , and the actual peak PV power generation value in the  $k$ th price period of the  $(i-1)$ st day, denoted by  $\text{Actual}_{i-1,k}$ . Please note that we must also capture and predict the seasonal change of the sunny day peak PV power generation values, while filtering out random

power decaying effects due to the presence of clouds. This is a smoothing operation. The  $\text{Predict}_{i,k}$  value is calculated as follows:

$$\text{Predict}_{i,k} = \beta(\text{Predict}_{i-1,k}, \text{Actual}_{i-1,k}) \cdot \text{Actual}_{i-1,k} + (1 - \beta(\text{Predict}_{i-1,k}, \text{Actual}_{i-1,k})) \cdot \text{Predict}_{i-1,k} \quad (9)$$

In the above equation, the learning rate function  $\beta(\text{Predict}_{i-1,k}, \text{Actual}_{i-1,k})$  is set to:

$$\beta_0, \quad \text{if } \text{Predict}_{i-1,k} < \text{Actual}_{i-1,k} \\ \beta_0 \cdot e^{-\lambda \cdot (\text{Predict}_{i-1,k} - \text{Actual}_{i-1,k})}, \quad \text{otherwise} \quad (10)$$

where  $\beta_0$  is the basis learning rate, and  $\lambda$  is the decaying parameter for the learning rate.

The motivation for this smoothing operation is as follows. Since (i) we want to predict the seasonal change of sunny day peak PV power generations while filtering out the effect of clouds and (ii)  $\text{Actual}_{i-1,k} \ll \text{Predict}_{i-1,k}$  only if there are clouds, it is natural that our new predicted sunny day peak PV power generation  $\text{Predict}_{i,k}$  should not be so much influenced by  $\text{Actual}_{i-1,k}$  (which is strongly affected by the clouds.) Therefore, we adopt the exponentially decaying learning rate function (10), rather than the constant learning rate in the original exponential average-based prediction algorithm.

The intra-day refinement phase of PV power generation prediction, which is performed at the start time of the  $k$ th ( $1 < k \leq 5$ ) price period of each day to predict the decay factors (and subsequently, the actual peak PV power generation values) in the remainder price periods, can be implemented via exactly the same algorithm (7) as the intra-day refinement phase of load power consumption prediction. Finally, in contrast to the load power consumption prediction, overestimating peak (or average) PV power generation needs to be avoided. Therefore similarly, we modify the intra-day refinement phase of peak PV power generation prediction as follows to avoid overestimating, in that after we derive the  $\text{Refine}_{i,\hat{k}}$  ( $2 \leq \hat{k} \leq 5$ ) value, we add the following conditional correction phase:

$$\text{Refine}_{i,\hat{k}} \leftarrow \text{Refine}_{i,\hat{k}} \cdot \eta_{\text{pv}}, \quad \text{if } \text{Refine}_{i,\hat{k}} < \text{Predict}_{i,\hat{k}} \quad (11)$$

in which the correction factor  $\eta_{\text{pv}} < 1$ . We effectively learn the optimal  $\eta_{\text{pv}}$  value using the learning technique, similar to the learning process of the optimal  $\eta_{\text{load}}$  value.

The reason for this modification is as follows. Experimental results show that overestimating peak PV power generation in the  $\hat{k}$ th price period of the  $i$ th day is very likely to happen when  $\text{Refine}_{i,\hat{k}} < \text{Predict}_{i,\hat{k}}$ .

#### IV. ADAPTIVE RESIDENTIAL STORAGE CONTROL ALGORITHM

In this section, we discuss the proposed residential storage control algorithm, which could effectively utilize the combination of PV power generation and load power consumption prediction results to minimize the total energy cost over each billing period. The proposed storage control algorithm is *hierarchical* in that it consists of a *global control tier* and a *local control tier*. The global control tier is performed at *each decision epoch* (to be precisely defined later) to “plan” for the future discharging and charging schemes of the energy storage for the rest of the day. The local control tier is performed locally and much more frequently at regular fixed-length timing intervals

called *time slots* as the controller operates to mitigate the effect of prediction error. In control theory, the global tier of the control algorithm is essentially a feedforward control, which is mostly optimization-based, whereas the local tier is a feedback control, which is mostly real-time control. The combination of feedforward control and feedback control can be a very effective control strategy. Detailed algorithms for the global control tier and the local control tier shall be described in Sections IV-A and IV-B, respectively. Before introducing such detailed algorithms, we first define the term “decision epoch” and explain the (brief) optimization objective at each decision epoch in the global tier of storage control algorithm.

Consider that we are currently in the  $i$ th day of a billing period (a month). Then the decision epochs in that day are defined to be the start times of each price periods of that day (excluding the 1st OP period), i.e.,  $t_{s,k}$  for  $1 < k \leq 5$ . At each decision epoch, the storage controller obtains information about the PV power generation and load power consumption profile characteristics (peak and average power) over the  $k$ th,  $(k+1)$ st,  $\dots$ , 5th price periods from the intra-day refinement phase of PV and load predictors performed just at that decision epoch  $t_{s,k}$ . The controller is going to globally “plan” the discharging and charging scheme of the storage in the remainder price periods of the day, making use of such predicted characteristics. Obviously, the “globally planned storage charging/discharging scheme” obtained at decision epoch  $t_{s,k}$  may be modified at the subsequent decision epoch  $t_{s,k+1}$ . Please note that the start time of the 1st OP period is not considered as a decision epoch. This is because the unit energy price in the 1st OP period is the lowest, and it is very unlikely to have a peak power demand to be drawn from the Grid during that price period. Hence during the 1st OP period, the storage system is being charged, instead of being discharged as in the following 1st LP, the HP, and the 2nd LP periods. Thus, we simply assume that the peak power demand to be drawn from the Grid, which may affect the monthly demand price, will not occur during the 1st OP period. Furthermore, we assume that the storage system will be (nearly) fully charged at the end of the 1st OP period (at time  $t_{s,2}$ ).

We use  $E_{i,k}$  to denote the available storage energy at decision epoch  $t_{s,k}$  of the  $i$ th day. We have  $E_{i,2} \approx E_{\text{full}}$  where  $E_{\text{full}}$  is the storage energy when fully charged, and  $E_{i,2} \geq E_{i,3} \geq E_{i,4} \geq E_{i,5}$ , since the storage is being discharged in the 1st LP, the HP, and the 2nd LP period.

The proposed storage control algorithm possess the following three adaptive features: i) The storage control algorithm utilizes the most up-to-date prediction results of PV and load power profiles from the intra-day refinement phase; ii) at each decision epoch  $t_{s,k}$ , the global tier of the storage control algorithm may adaptively modify the optimization results for the rest of the day obtained at the former decision epoch  $t_{s,k-1}$ ; iii) the feedback control-based local tier is performed much more frequently to adaptively mitigate the effect of prediction error and the inaccuracy of the global tier.

#### A. The Global Control Tier

In contrast to the other parts of the paper, we use a continuous-time based system model in the description of the global control tier of the proposed storage control algorithm. The reason for using a continuous-time model is to effectively incorporate the PV and load prediction results in the global control tier and formulate the global control tier as a convex optimization problem. Consider that we are currently at decision epoch  $t_{s,k_0}$

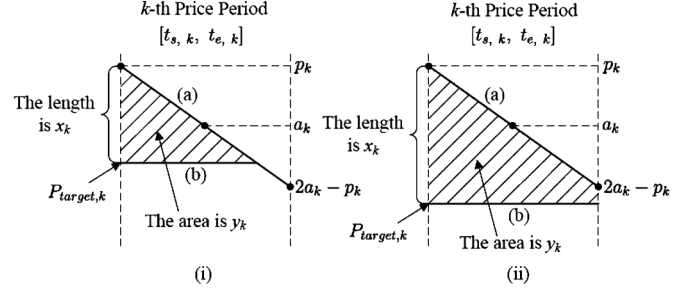


Fig. 2. Relationship between the predicted net load power, storage output power, and grid power profiles in the  $k$ th price period of the  $i$ th day. Fig. 2 (i) corresponds to the case when  $P_{\text{target},k} \geq 2a_k - p_k$  ( $x_k \leq 2p_k - 2a_k$ ). Fig. 2 (ii) corresponds to the case when  $P_{\text{target},k} < 2a_k - p_k$  ( $x_k > 2p_k - 2a_k$ ).

( $1 < k_0 \leq 5$ ) of the  $i$ th day. In this algorithm, let  $P_{\text{net},i}(t)$ ,  $t \in [t_{s,k_0}, t_{e,5} = 24 : 00]$  denote the predicted *net load* power consumption profile of the rest of the  $i$ th day, which equals to the predicted load power consumption profile minus the predicted PV power generation profile. Such predicted  $P_{\text{net},i}(t)$  profile can be reconstructed from the intra-day refinement phase of PV and load peak and average power predictions, and the details of reconstruction shall be discussed later. The storage output power, which is the control variable of the global tier of the storage control algorithm, is denoted by  $P_{\text{st},i}(t)$ . Therefore, the (predicted) power drawn from the smart grid (i.e., the grid power), denoted by  $P_{\text{grid},i}(t)$ , can be calculated via  $P_{\text{grid},i}(t) = P_{\text{net},i}(t) - P_{\text{st},i}(t)$ .

Consider a specific price period (the  $k$ th price period with  $1 < k \leq 5$ , for instance) of the  $i$ th day, as shown in Fig. 2. We use  $p_k$  and  $a_k$  to denote the predicted peak and average net load power consumption values in that price period, respectively. Furthermore, we use  $p_{\text{load},k}$  and  $a_{\text{load},k}$  to denote the predicted peak and average load power consumption values, and use  $p_{\text{pv},k}$  and  $a_{\text{pv},k}$  to denote the predicted peak and average PV power generation values, respectively, over the  $k$ th price period of the  $i$ th day. Please note that the index  $i$  of such  $p_k$ ,  $a_k$ , etc. values has been omitted for the conciseness in notation. We obtain the above-defined  $p_{\text{load},k}$ ,  $a_{\text{load},k}$ ,  $p_{\text{pv},k}$ , and  $a_{\text{pv},k}$  values from the intra-day refinement phase of PV and load predictions, and approximately calculate the  $p_k$  and  $a_k$  values in the following way:

$$\begin{aligned} p_k &= p_{\text{load},k} - (2a_{\text{pv},k} - p_{\text{pv},k}) \\ a_k &= a_{\text{load},k} - a_{\text{pv},k} \end{aligned} \quad (12)$$

The intuitions of (12) are given as follows: The predicted peak net load power consumption  $p_k$  should be equal to the predicted peak load power consumption  $p_{\text{load},k}$  subtracted by the minimum PV power generation, which is approximated by  $2a_{\text{pv},k} - p_{\text{pv},k}$ . Similarly,  $a_k$  should be equal to the predicted average load power consumption  $a_{\text{load},k}$  subtracted by the average PV power generation  $a_{\text{pv},k}$ .

We assume that the net load power consumption during the  $k$ th ( $1 < k \leq 5$ ) price period of the  $i$ th day, i.e.,  $P_{\text{net},i}(t)$ ,  $t \in [t_{s,k}, t_{e,k}]$ , is uniformly distributed between the lowest value  $2a_k - p_k$  and the highest value  $p_k$ . Without loss of generality, we draw such predicted net load power consumption curve as line segment (a) in Fig. 2. Please note that although Fig. 2 arranges the net load power consumption during the  $k$ th price period in descending order from the left side, it does not show the exact time series variation of the net load but the distribution of the net load during this price period.

Briefly speaking, the role of storage discharging in the price period of interest is to make the power drawn from the Grid,  $P_{\text{grid},i}(t)$ , lower than the net load power consumption  $P_{\text{net},i}(t)$ . Let  $y_k$  denote the predicted amount of energy drawn from the storage system during the  $k$ th price period. For a given  $y_k$ , we prove<sup>1</sup> that the optimal (predicted) grid power profile for peak (or cost) minimization is given by  $\min(P_{\text{net},i}(t), P_{\text{target},k})$  for  $t \in [t_{s,k}, t_{e,k}]$  shown as curve (b) in Fig. 2, where  $P_{\text{target},k}$  is the maximum (predicted) grid power during this price period (also shown in Fig. 2.) Please notice that Fig. 2(i) and (ii) correspond to the cases when  $P_{\text{target},k} \geq 2a_k - p_k$  and  $P_{\text{target},k} < 2a_k - p_k$ , respectively. The relationship between  $y_k$  and  $P_{\text{target},k}$  are provided as follows: Let  $x_k = p_k - P_{\text{target},k}$ , and then we have

$$y_k = \frac{1}{2} \cdot x_k \cdot \frac{x_k \cdot (t_{e,k} - t_{s,k})}{2p_k - 2a_k} = \frac{(x_k)^2 \cdot (t_{e,k} - t_{s,k})}{4(p_k - a_k)} \quad (13)$$

when  $P_{\text{target},k} \geq 2a_k - p_k$  ( $x_k \leq 2p_k - 2a_k$ ) as shown in Fig. 2(i). On the other hand, the function is given by

$$y_k = \frac{(2x_k - 2p_k + 2a_k) \cdot (t_{e,k} - t_{s,k})}{2} = (x_k - p_k + a_k) \cdot (t_{e,k} - t_{s,k}) \quad (14)$$

when  $P_{\text{target},k} < 2a_k - p_k$  ( $x_k > 2p_k - 2a_k$ ) as shown in Fig. 2(ii). Equations (13) and (14) are derived based on the observation that  $y_k$  is the area of the shadowed triangle (Fig. 2(i)) or trapezoid (Fig. 2(ii)) with the height  $t_{e,k} - t_{s,k}$ .

The above-defined  $x_k$  denotes the maximum power reduction between the predicted net load power profile and the predicted grid power profile in the  $k$ th price period. We use  $x_k$  as the optimization variable in the global control tier instead of  $P_{\text{target},k}$  in order to formulate the global tier as a convex optimization problem. The relationship between  $y_k$  and  $x_k$ , denoted by  $y_k = f_k(x_k)$ , is already provided in (13) and (14). In fact,  $y_k$  is a *convex* and *monotonically increasing* function of  $x_k$ , because: i)  $(df_k(x_k))/(dx_k) > 0$ , and ii)  $(df_k(x_k))/(dx_k)$  is the smallest at the beginning ( $x_k = 0$ ), and then gradually increases as  $x_k$  becomes larger. One can see that capturing the relationship between  $x_k$  and  $y_k$  necessitates the usage of the continuous-time model in the global control tier.

Now we return to the optimal storage control problem at decision epoch  $t_{s,k_0}$  ( $1 < k_0 \leq 5$ ) of the  $i$ th day, as illustrated in Fig. 3 ( $k_0 = 3$  in this case.) At that time, we derive the predicted  $p_k$  and  $a_k$  values for  $k_0 \leq k \leq 5$  from the intra-day refinement phase of PV power generation and load power consumption predictions at decision epoch  $t_{s,k_0}$ , as well as (12). The storage energy at decision epoch  $t_{s,k_0}$  is given by  $E_{i,k_0}$ . We use  $\text{Peak}_{\text{OP}}$ ,  $\text{Peak}_{\text{LP}}$ , and  $\text{Peak}_{\text{HP}}$ , respectively, to denote the actual peak grid power consumption values *observed so far* over the OP, LP, and HP price periods in this billing period. Such  $\text{Peak}_{\text{OP}}$ ,  $\text{Peak}_{\text{LP}}$ , and  $\text{Peak}_{\text{HP}}$  values are initialized to be zero at the beginning of each billing period. The  $x_k$  values for  $k_0 \leq k \leq 5$  in this optimal storage control problem are optimization variables, and we have  $y_k = f_k(x_k)$  for  $k_0 \leq k \leq 5$ . The objective of the optimal storage control problem is to find the optimal  $x_k$  values for  $k_0 \leq k \leq 5$ , subject to the storage energy constraint  $\sum_{k=k_0}^5 y_k \leq E_{i,k_0}$ , so as to minimize the total cost over the billing period.

Then the proposed (near-) optimal storage control algorithm at decision epoch  $t_{s,k_0}$  is given by the following. First we check whether the storage system has enough energy for peak

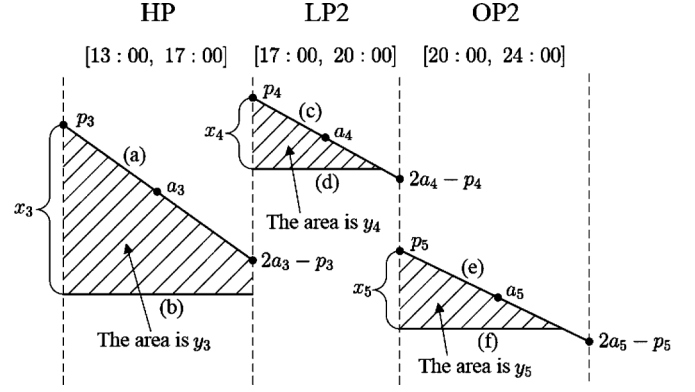


Fig. 3. The optimal control problem at decision epoch  $t_{s,3} = 13:00$ .

shaving such that the (predicted) cost due to demand price in the billing period will not increase in the  $i$ th day, or in other words, the (predicted) power profile drawn from the Grid,  $P_{\text{grid},i}(t)$ , will not exceed the  $\text{Peak}_{\text{LP}}$ ,  $\text{Peak}_{\text{HP}}$ , and  $\max(\text{Peak}_{\text{OP}}, \text{Peak}_{\text{LP}}, \text{Peak}_{\text{HP}})$  values in the LP, HP, and OP price periods in the rest of the  $i$ th day, respectively. We know that the demand price is the dominating factor over the unit energy price in [9]. More specifically, we set:

$$x_2 \leftarrow \max(0, p_2 - \text{Peak}_{\text{LP}}), \quad \text{if } k_0 = 2 \quad (15)$$

$$x_3 \leftarrow \max(0, p_3 - \text{Peak}_{\text{HP}}), \quad \text{if } k_0 \leq 3 \quad (16)$$

$$x_4 \leftarrow \max(0, p_4 - \text{Peak}_{\text{LP}}), \quad \text{if } k_0 \leq 4 \quad (17)$$

$$x_5 \leftarrow \max(0, p_5 - \max(\text{Peak}_{\text{OP}}, \text{Peak}_{\text{LP}}, \text{Peak}_{\text{HP}})) \quad (18)$$

Then we compare  $E_{i,k_0}$  and  $\sum_{k=k_0}^5 y_k = \sum_{k=k_0}^5 f_k(x_k)$ , and we have the following two cases based on the comparison results.

1) *Case I* ( $E_{i,k_0} \geq \sum_{k=k_0}^5 f_k(x_k)$ ): In this case, the storage energy is adequate for peak shaving such that the (predicted) cost due to demand price in the billing period will not increase in the rest of the  $i$ th day. We further minimize the (predicted) cost due to unit energy price in the rest of the  $i$ th day, subject to the constraint that the (predicted) cost due to demand price will not increase in this day. We call such problem *cost minimization with adequate energy* (CMAE), with deterministic solution as follows:

1) If  $k_0 = 2$ , let  $x_3 \leftarrow f_3^{-1}(E_{i,2} - f_2(x_2) - f_4(x_4) - f_5(x_5))$ . Then  $x_3$  will become larger than its original value  $\max(0, p_3 - \text{Peak}_{\text{HP}})$ . We keep the  $x_2, x_4$ , and  $x_5$  values the same as before. This is because the unit energy price in the HP period is the highest among each day, and thereby, we are going to use all the (predicted) surplus storage energy in the HP period for total cost minimization.

2) If  $k_0 = 3$ , we set  $x_3 \leftarrow f_3^{-1}(E_{i,3} - f_4(x_4) - f_5(x_5))$ , and keep the  $x_4$  and  $x_5$  values unchanged.

3) If  $k_0 = 4$ , we set  $x_4 \leftarrow f_4^{-1}(E_{i,4} - f_5(x_5))$ , and keep the  $x_5$  value the same as before.

4) If  $k_0 = 5$ , we simply leave the  $x_5$  value as it was. This is because the unit energy price in the 2nd OP price period is the lowest among each day, and thus, spending additional storage energy in this price period will have no benefit.

2) *Case II* ( $E_{i,k_0} < \sum_{k=k_0}^5 f_k(x_k)$ ): In this case, the storage energy is not adequate for peak shaving and therefore, we have to make the predicted peak grid power consumption over *at least* one of the LP, HP, and OP price periods of the  $i$ th day exceed

<sup>1</sup>Please refer to the Appendix for the detailed proof.

the  $\text{Peak}_{\text{LP}}$ ,  $\text{Peak}_{\text{HP}}$ , and  $\max(\text{Peak}_{\text{OP}}, \text{Peak}_{\text{LP}}, \text{Peak}_{\text{HP}})$  values, respectively. We solve the following optimization problem, called the *peak shaving with inadequate energy* (PSIE) problem, such that the (predicted) cost increase due to demand price in the  $i$ th day will be minimized.

---

### The PSIE Optimization Problem

---

**Find** the optimal values  $x_k$  for  $k_0 \leq k \leq 5$ .

**Minimize:**

$$\begin{aligned} & \text{Price}_{D_{\text{LP}}} \cdot \max\{\text{Peak}_{\text{LP}}, \mathbf{I}[k_0 = 2](p_2 - x_2), \\ & \mathbf{I}[k_0 \leq 4](p_4 - x_4)\} \\ & + \text{Price}_{D_{\text{HP}}} \cdot \max\{\text{Peak}_{\text{HP}}, \mathbf{I}[k_0 \leq 3] \cdot (p_3 - x_3)\} \\ & + \text{Price}_{D_{\text{Overall}}} \cdot \max\{\text{Peak}_{\text{LP}}, \text{Peak}_{\text{HP}}, \text{Peak}_{\text{OP}}, \mathbf{I}[k_0 = 2] \\ & \cdot (p_2 - x_2), \mathbf{I}[k_0 \leq 3](p_3 - x_3), \mathbf{I}[k_0 \leq 4](p_4 - x_4), p_5 - x_5\} \end{aligned} \quad (19)$$

in which  $\mathbf{I}[x]$  is the indicator function, which equals to one if statement  $x$  is true, and equals to zero otherwise.

**Subject to:**

$$x_k \geq 0, \quad \text{for } k_0 \leq k \leq 5 \quad (20)$$

$$\sum_{k=k_0}^5 f_k(x_k) \leq E_{i,k_0} \quad (21)$$

Remember that  $f_k(x_k)$  is a convex and monotonically increasing function over  $x_k$  for  $k_0 \leq k \leq 5$ . The above PSIE problem is a convex optimization problem since it has convex objective function and convex inequality constraints, and thus, it can be optimally solved with polynomial time complexity by using standard convex optimization techniques such as [12].

### B. The Local Control Tier

The local control tier of the storage control algorithm is performed along with system operation to compensate for the errors in the PV power generation and (or) load power consumption predictions. In this part, we return to the slotted time model as described in Section II.

Consider that we are currently at the  $j$ th time slot, which belongs to the  $k$ th price period, of the  $i$ th day of a billing period. At that time, we have derived the  $P_{\text{target},k}$  value from the global tier of the storage control algorithm performed at decision epoch  $t_{s,k}$ . We also have the actual net load power consumption  $P_{\text{net},i}[j] = P_{\text{load},i}[j] - P_{\text{pv},i}[j]$ . The basic job of the local tier of the storage control algorithm is: trying to limit the grid power, given by  $P_{\text{grid},i}[j] = P_{\text{net},i}[j] - P_{\text{st},i}[j]$ , no more than the  $P_{\text{target},k}$  value through controlling the storage output power  $P_{\text{st},i}[j]$ . Moreover, the local tier should also make sure that the physical limitations of the storage system are not violated, i.e., the amount of energy stored in the storage system cannot exceed the maximum value  $E_{\text{full}}$  or become less than zero at the end of the  $j$ th time slot. Details of the local tier of storage control algorithm are given as follows:

## V. EXPERIMENTAL RESULTS

In this section, we present the experimental results on load power consumption and PV power generation prediction algorithms proposed for the residential smart grid users, as well as

---

### Algorithm 1: Local tier of storage controller at time slot $j$ , price period $k$ , day $i$ .

---

Assume that at the beginning of the  $j$ th time slot, the amount of stored energy in the storage system is  $E_i[j]$ .

**If**  $P_{\text{net},i}[j] > P_{\text{target},k}$ :

$$P_{\text{st},i}[j] \leftarrow \min(P_{\text{net},i}[j] - P_{\text{target},k}, \frac{E_i[j]}{D}).$$

**Else If** we are currently at the 2<sup>nd</sup> OP period, i.e.,  $k = 5$ :

$$P_{\text{st},i}[j] \leftarrow \max(P_{\text{net},i}[j] - P_{\text{target},k}, -\frac{E_{\text{full}} - E_i[j]}{D}).$$

//This is because the unit energy price in the 2<sup>nd</sup> OP period is the lowest. We may charge the storage system in the 2<sup>nd</sup> OP period, as long as the grid power  $P_{\text{grid},i}[j] = P_{\text{net},i}[j] - P_{\text{st},i}[j]$  is no more than  $P_{\text{target},k}$ .

**Else**  $P_{\text{st},i}[j] \leftarrow 0$ .

Set  $P_{\text{target},k} \leftarrow \max(P_{\text{target},k}, P_{\text{net},i}[j] - P_{\text{st},i}[j])$ .

---

the effectiveness of the proposed residential storage control algorithm. In the experiments, we use the electric load data from the Baltimore Gas and Electric Company measured in the year 2007 [11]. We use PV power generation profiles measured at (i) Duffield, VA, measured in the year 2007, and (ii) Los Angeles, CA, measured in the year 2012 [13]. These two profiles are representative of the PV generation profiles in the west coast and the east coast of the U.S., respectively.

### A. Load and PV Power Profile Predictions

In this section, we show some representative experimental results on the accuracy of the peak load power consumption and PV power generation predictions. The average load power consumption and PV power generation prediction results are in general 10%–15% more accurate than the peak predictions, and are therefore not shown due to space limitation.

Fig. 4 compares the peak load power consumption prediction results and the actual peak load power consumption results in the HP period of each day in a year. The peak load power consumption prediction results shown in the top subfigure come from the initial prediction performed at time 00:00 of each day, whereas the prediction results in the bottom subfigure come from the intra-day refinement performed at time  $t_{s,3} = 13 : 00$ . Data in the first 120 days of the year are used for initial training, and thus the prediction results over those days are not shown in Fig. 4. We can observe from Fig. 4 that the proposed adaptive regression-based initial prediction algorithm is effective in load power consumption prediction, resulting in an average prediction error of about 8%, by making use of both the daily and weekly dependencies. The average prediction error is further reduced to less than 4%, i.e., less than 50% of the average prediction error in initial prediction, by the effective use of intra-day refinement.

Fig. 5 compares the peak PV power generation prediction results with the actual PV power generation results in the 1st LP period of each day in a year, using the PV data measured at Duffield, VA, USA. The peak PV power generation prediction results shown in the top subfigure come from the initial prediction performed at time 00:00 of each day, whereas the prediction results shown in the bottom subfigure come from the intra-day refinement procedure performed at time  $t_{s,2} = 10 : 00$ . Data in the first 90 days in the year are used for initial training, and thus the prediction results over those days are not shown in

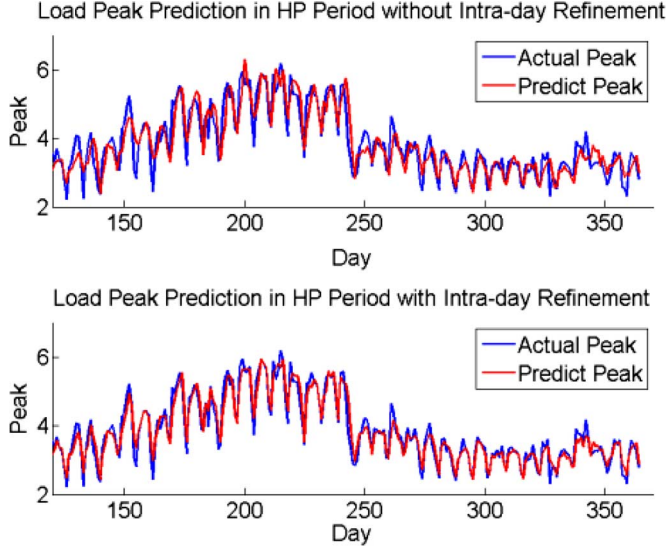


Fig. 4. Comparison between the peak load power consumption prediction results from initial prediction (top) and from intra-day refinement at time  $t_{s,3} = 13:00$  (bottom) and actual peak load power consumption results.

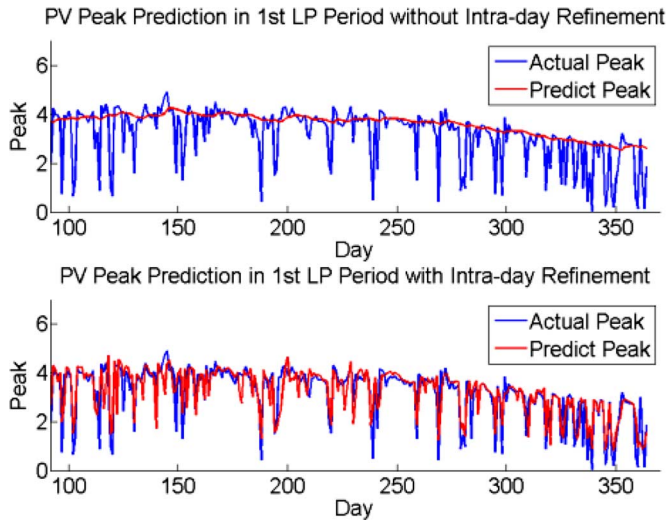


Fig. 5. Comparison between the peak PV power generation prediction results from the initial prediction (top) and from intra-day refinement at time  $t_{s,2} = 10:00$  (bottom) and actual peak PV power generation results.

Fig. 5. We can observe that the proposed modified exponential average-based initial prediction algorithm is effective in predicting the sunny day peak (and also average) PV power generation over each day in a year, by effectively capturing the long-term seasonal change of sunny day peak power generation values throughout a year while filtering out the random effects of clouds. The proposed intra-day refinement technique also proves itself effective in predicting the decay factors due to clouds by reducing the average prediction error to about 14%. We achieve even more accurate peak PV power generation predictions on PV data measured at Los Angeles, CA, USA, with an average error of less than 12%.

### B. The Proposed Residential Storage Control Algorithm

In our experiments for testing the effectiveness of the proposed residential storage control algorithm, the residential smart grid user is equipped with the load devices and PV system with

power consumption and generation profiles same as the profiles used in Section V-A, as well as the storage system for peak shaving. We define the *cost saving capability* of a storage control algorithm (the proposed algorithm or the baseline algorithm) to be the average monthly cost saving due to the additional storage system, compared to the same residential smart grid user equipped only with the PV system. We compare the cost saving capabilities of the proposed near-optimal storage control algorithm with three baseline algorithms. All the baseline algorithms charge the storage system from the Grid during the OP period with constant power. The first baseline algorithm is a relatively simple algorithm that distributes all the available energy stored in the storage system evenly in the HP and LP periods that have relatively higher monthly demand price and unit energy price. The second baseline algorithm is a relatively more advanced algorithm that distributes its available energy with constant output power  $P_{st,HP}^{Base2}$  in the HP period and  $P_{st,LP}^{Base2}$  in the LP period. The  $P_{st,HP}^{Base2}$  and  $P_{st,LP}^{Base2}$  values satisfy:

$$P_{st,HP}^{Base2} / P_{st,LP}^{Base2} = \text{Price}_{D_{HP}} / \text{Price}_{D_{LP}} \quad (22)$$

The third baseline algorithm, on the other hand, distributes the available energy of the storage system during the HP and LP periods trying not to increase the  $\text{Peak}_{LP}$ ,  $\text{Peak}_{HP}$ , and  $\max(\text{Peak}_{OP}, \text{Peak}_{LP}, \text{Peak}_{HP})$  values. More specifically, during each billing period, the third baseline algorithm maintains the three peak values observed from the beginning of the billing period. Suppose we are at time slot  $j$  of the  $i$ th day, which belongs to the HP or LP periods. The storage will provide power  $P_{net,i}[j] - \text{Peak}_{HP}$  (or  $P_{net,i}[j] - \text{Peak}_{LP}$ ) if the net load power  $P_{net,i}[j] > \text{Peak}_{HP}$  (or  $P_{net,i}[j] > \text{Peak}_{LP}$ ) and the storage has enough energy. Otherwise, the storage will not supply power. The objective is to maintain the grid power in this time slot not to exceed the  $\text{Peak}_{HP}$  (or  $\text{Peak}_{LP}$ ) and the  $\max(\text{Peak}_{OP}, \text{Peak}_{LP}, \text{Peak}_{HP})$  values.

Fig. 6 shows the comparison results on the cost saving capabilities between the proposed storage control algorithm and the baseline algorithms. The x-axis of this figure is the total storage capacity, and the y-axis is the ratio of the cost saving capability of a storage control algorithm (the proposed algorithm or the baseline algorithm) to the cost saving capability of the proposed near-optimal algorithm. We can see from Fig. 6 that the proposed near-optimal residential storage control algorithm consistently outperforms the three baseline systems, with an average cost saving capability improvement of 58.6%, 33.2%, and 89.8% than the first, second, and third baseline algorithms, respectively. Compared with Baseline 1 and Baseline 2, the proposed algorithm achieves higher improvement in Fig. 6(a) when the storage capacity is relatively large, whereas it achieves higher improvement in Fig. 6(b) when the storage capacity is relatively small. In addition, Baseline 3 achieves relatively higher performance in Fig. 6(b) when the PV generation profile measured at Los Angeles is used. These observations imply that the results are affected by the dataset and the condition.

Finally, we analyze the effect of the correction factor  $\eta_{load}$  (defined in Section III) on the cost saving capability of the storage controller, in order to demonstrate the necessity of avoiding under-estimation of load power consumption. We analyze the effect of  $\eta_{pv}$  in the same manner, with details omitted due to space limitation. The learning results show that the optimal  $\eta_{load} \approx 1.1$  (the optimal  $\eta_{pv} \approx 0.9$ .) We

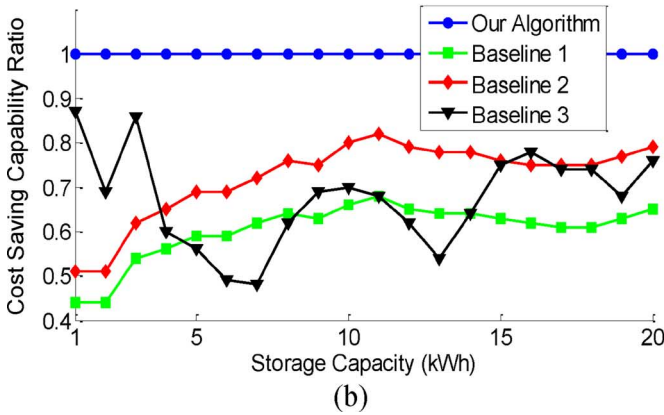
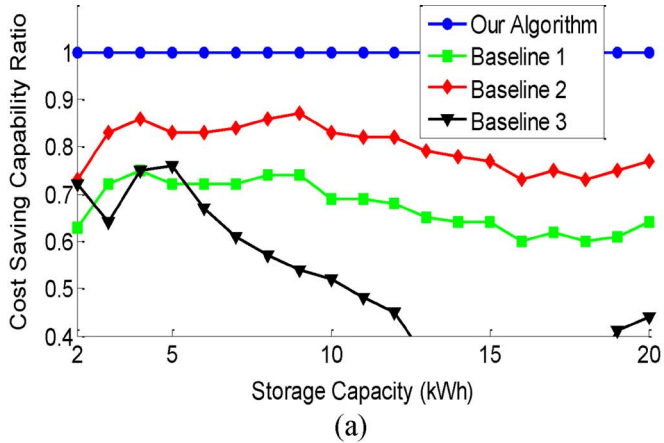


Fig. 6. Comparison of the cost saving capabilities between the proposed near-optimal storage control algorithm and baseline algorithms: (a) we use the PV generation profile measured at Duffield, VA, USA, and (b) we use the PV generation profile measured at Los Angeles, CA, USA.

TABLE I  
COMPARISON OF NORMALIZED COST SAVING CAPABILITIES OF THE PROPOSED STORAGE CONTROL ALGORITHM AT DIFFERENT  $\eta_{load}$  VALUES

$\eta_{load}$	0.85	0.9	0.95	1.0	1.05
Cost Saving	68.2%	76.3%	87.3%	93.5%	99.3%
$\eta_{load}$	1.1	1.15	1.2	1.25	1.3
Cost Saving	1	99.1%	92.2%	80.0%	65.4%

provide the normalized cost saving capabilities of the storage controller under different  $\eta_{load}$  values in Table I. One can observe that the cost saving capability of the proposed storage control algorithm degrades both when  $\eta_{load} > 1.1$  and when  $\eta_{load} < 1.1$ , but the sensitivity on the  $\eta_{load}$  value is not very high when  $1.05 < \eta_{load} < 1.15$ . However, when  $\eta_{load} > 1.15$  or  $\eta_{load} < 1.05$ , the performance degradation becomes significant. We can see that both under-estimation ( $\eta_{load} < 1.0$ ) and large over-estimation ( $\eta_{load} > 1.15$ ) of the load power consumption will result in significant degradation in the cost saving capability. However, the performance degradation due to under-estimation is in general more significant than that due to over-estimation. For example, the performance degradation when  $\eta_{load} = 0.9$  is comparable with that when  $\eta_{load} = 1.25$ , whereas the performance degradation when  $\eta_{load} = 0.85$  is comparable with that when  $\eta_{load} = 1.3$ .

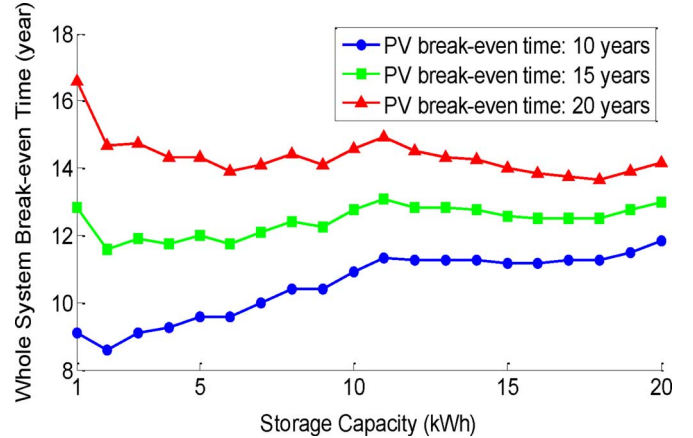


Fig. 7. Break-even time of the whole PV and storage system for the residential smart grid user as a function of storage capacity.

### C. Break-Even Time Analysis

We analyze the break-even time of the whole PV and storage system. In this analysis, the PV module has a fixed peak power generation capacity (when the solar irradiance is  $1000 \text{ W/m}^2$ ) of  $2.5 \text{ kW}$ , and we find the optimal storage capacity to reduce the break-even time of the whole system. Since the PV module and storage module have different life times ( $\sim 20$  years for the PV module and  $\sim 2.5$  years/500–800 cycles for lead-acid batteries [14]), we define the break-even time of the whole system as follows. We use the least common multiple (20 years) of the life times of PV and storage modules as the life time of the whole system. During this operation period, we need to replace the batteries in the storage system eight times. Let  $Total\_Cost$  denote the total cost of the whole PV and storage system in its 20-year life time, including the replacement cost of the battery-based storage system. Let the break-even time of the whole PV and storage system denote the time required for the residential smart grid user to saving  $Total\_Cost$  amount of electricity cost. We use  $\$50/\text{kWh}$  as the unit cost of the storage system, which is similar to [14]. Due to different PV technologies, we use different break-even time values of the PV module: 10 years, 15 years, and 20 years, corresponding to different prices of the PV module  $\$1980$ ,  $\$2970$ , and  $\$3960$ , respectively. With these different break-even time values of the PV module, we analyze the break-even time of the whole system under different storage module sizes as shown in Fig. 7.

We derive the following conclusions from Fig. 7: i) In all of the three cases, the incorporation of the storage module can reduce the break-even time of the whole system by up to 30% compared with the case when only the PV module is installed. ii) When the PV break-even time is 10 years and is relatively low, the most desirable size of the storage module is low (2 kWh). This is because a small-size storage module can effectively store the excessive PV power generation and use it for peak shaving and demand cost reduction. On the other hand, a large-size storage module, which has a larger break-even time than the PV module, will actually increase the break-even time of the whole system. We can also observe from Fig. 7 that the break-even time of the whole system is less sensitive to the storage module size when the PV break-even time is 15 years or 20 years and is comparable with the break-even time of the storage system itself. We may perform other optimizations, e.g., finding the optimal sizes of the PV module and storage module

with a given budget, which is not elaborated in this work due to space limitation.

## VI. CONCLUSION

This paper addresses the problem on integrating residential PV and storage systems into the smart grid for simultaneous peak shaving and total electricity cost minimization, making use of the dynamic energy pricing models. We first propose novel PV power generation and load power consumption profile forecasting methods, which are specifically developed for the residential storage controller for performing peak shaving. Moreover, we propose an effective residential storage control algorithm, which consists of a global control tier performed at each decision epoch of a billing period to globally “plan” the future discharging/charging schemes of the storage system, and a local control tier performed along with system operation to compensate for the prediction errors. We find the optimal size of the energy storage so as to minimize the break-even time of the initial investment in the PV and storage systems. Experimental results demonstrate that the proposed residential storage control algorithm saves at most 89.8% more electricity cost than the baseline algorithms.

## APPENDIX

We use proof by contradiction. Consider some other (predicted) grid power profile  $P'_{\text{grid}}(t)$  that results in the same  $y_k$  value. The total cost induced by the energy price component is the same in the  $k$ th price period (because  $y_k$  is the same.) Suppose  $P'_{\text{grid}}(t) < P_{\text{target},k}$  for  $t \in [t_{s,k}, t_{e,k}]$ , which will result in a smaller (predicted) peak power level in this price period. Of course we also have  $P'_{\text{grid}}(t) \leq P_{\text{net},i}(t)$ . Then the (predicted) total amount of energy drawn from the grid in the  $k$ th price period is given by  $\int_{t_{s,k}}^{t_{e,k}} (P_{\text{net},i}(t) - P'_{\text{grid}}(t))dt$  and is larger than  $y_k = \int_{t_{s,k}}^{t_{e,k}} (P_{\text{net},i}(t) - \min(P_{\text{net},i}(t), P_{\text{target},k}))dt$ . We have found the contradiction and have proved the statement.

## REFERENCES

- [1] L. D. Kannberg, D. P. Chassin, J. G. DeSteele, S. G. Hauser, M. C. Kintner-Meyer, R. G. Pratt, L. A. Schienbein, and W. M. Warwick, “GridWise™: The benefits of a transformed energy system,” PNNL-14396, Pacific Northwest National Laboratory. Richland, WA, USA, Sep. 2003.
- [2] S. M. Amin and B. F. Wollenberg, “Toward a smart grid: Power delivery for the 21st century,” *IEEE Power Energy Mag.*, vol. 3, no. 5, pp. 34–41, 2005.
- [3] S. Caron and G. Kesidis, “Incentive-based energy consumption scheduling algorithms for the smart grid,” in *Proc. Smart Grid Commun. (SmartGridComm) Conf.*, 2010.
- [4] Y. Kim, N. Chang, Y. Wang, and M. Pedram, “Maximum power transfer tracking for a photovoltaic-supercapacitor energy system,” in *Proc. ISLPED*, 2010.
- [5] Y. Wang, S. Yue, L. Kitabayashi, S. Deshpande, and M. Pedram, “A hierarchical control algorithm for managing electrical energy storage systems in homes equipped with PV power generation,” in *Proc. IEEE Green Technol. Conf.*, 2012.
- [6] T. Hiyama and K. Kitabayashi, “Neural network based estimation of maximum power generation from PV module using environmental information,” *IEEE Trans. Energy Convers.*, vol. 12, no. 3, pp. 241–247, 1997.
- [7] C. Chen, B. Das, and D. J. Cook, “Energy prediction based on resident’s activity,” in *Proc. SensorKDD’10*.
- [8] L. Wei and Z.-H. Han, “Short-term power load forecasting using improved ant colony clustering,” in *Proc. WKDD*, 2008.
- [9] Los Angeles Department of Water & Power, Electric Rates [Online]. Available: <http://www.ladwp.com/ladwp/cms/ladwp001752.jsp>
- [10] C. M. Bishop, *Pattern Recognition and Machine Learning*. New York: Springer, Aug. 2006.
- [11] Baltimore Gas and Electric Company, Historical Load Data [Online]. Available: [https://supplier.bge.com/LoadProfiles\\_EnergySettlement/historicalloaddata.htm](https://supplier.bge.com/LoadProfiles_EnergySettlement/historicalloaddata.htm)
- [12] M. Grant and S. Boyd, “CVX: Matlab software for disciplined convex programming, version 1.21,” [Online]. Available: <http://cvxr.com/cvx> Feb. 2011
- [13] Solar Resource & Meteorological Assessment Project (SOLRMAP) [Online]. Available: <http://www.nrel.gov/mide/lmu/>
- [14] D. Zhu, Y. Wang, S. Yue, Q. Xie, N. Chang, and M. Pedram, “Maximizing return on investment of a grid-connected hybrid electrical energy storage system,” in *Proc. ASP-DAC*, 2013.



**Yanzhi Wang** (S’12) received the B.S. degree with distinction in electronic engineering from Tsinghua University, Beijing, China, in 2009. He is currently pursuing the Ph.D. degree in electrical engineering at University of Southern California, Los Angeles, CA, USA, under the supervision of Prof. Massoud Pedram. His current research interests include system-level power management, next-generation energy sources, hybrid electrical energy storage systems, near-threshold computing, cloud computing, mobile devices and smartphones, and the smart grid.

He has published around 70 papers in these areas.



**Xue Lin** (S’12) received the B.S. degree from Tsinghua University, Beijing, China, in 2009. She is now a Ph.D. student in the Department of Electrical Engineering at University of Southern California, Los Angeles, CA, USA. Her advisor is Prof. Massoud Pedram. She has been working on power management of photovoltaic (PV) systems, near-threshold computing of FinFET circuits, and power management of energy storage systems. She has published more than 20 papers in these areas.



**Massoud Pedram** (F’01) received a Ph.D. in electrical engineering and computer sciences from the University of California, Berkeley, CA, USA, in 1991. He is the Stephen and Etta Varra Professor in the Ming Hsieh Department of Electrical Engineering at University of Southern California, Los Angeles, CA, USA. He holds 10 U.S. patents and has published four books, 12 book chapters, and more than 130 archival and 340 conference papers. His research ranges from low power electronics, energy-efficient processing, and cloud computing

to photovoltaic cell power generation, energy storage, and power conversion, and from RT-level optimization of VLSI circuits to synthesis and physical design of quantum circuits. For this research, he and his students have received six conference and two IEEE Transactions Best Paper Awards. Dr. Pedram is a recipient of the 1996 Presidential Early Career Award for Scientists and Engineers, a Fellow of the IEEE, an ACM Distinguished Scientist, and currently serves as the Editor-in-Chief of the *ACM Transactions on Design Automation of Electronic Systems* and the *IEEE JOURNAL ON EMERGING AND SELECTED TOPICS IN CIRCUITS AND SYSTEMS*. He has also served on the technical program committee of a number of premiere conferences in his field and was the founding Technical Program Co-chair of the 1996 International Symposium on Low Power Electronics and Design and the Technical Program Chair of the 2002 International Symposium on Physical Design.